DOI 10.24425/aee.2024.149927

Influence of electromagnetic transient physical models considering characterization characteristics on capacitive voltage transformers

JIE GENG, HAIYONG YANG, YI LI, XIAO ZHANG, YIHANG WANG✉

Office of Construction and Campus Planning, Tsinghua University
Beijing 100084, China

e-mail: {yanghaiyon/yi-1}@mail.tsinghua.edu.cn, zxlove008@126.com,
{wording_5050/✉ yihang_w12}@163.com

(Received: 29.11.2023, revised: 18.04.2024)

Abstract: The equivalent circuit of traditional capacitive voltage transformers often faces the problem of complex data calculation and difficulty in grasping the internal nonlinear characteristics of transformers when constructing broadband models, resulting in poor power accuracy and stability. Therefore, with the help of electromagnetic transient physical models, the admittance sub model and nonlinear model are established by considering the frequency and saturation characteristics of the transformer. Based on the characteristics of capacitive voltage transformers, the model is processed in parallel to obtain a broadband coupling transformer model. The results showed that the error between the simulated current peak amplitude and voltage results of the model and the measured values was less than 2% and 1%, respectively. In the fault results, the harmonic error of the load voltage of the improved transformer was relatively small, far less than the error result of 2.73% of the traditional transformer. The proposed transformer model can better characterize its characteristics and has good transient response ability, providing reference tools and value for the operation and state detection of power systems.

Key words: broadband admittance parameters, capacitive voltage transformer, electromagnetic transient model, excitation deviation, saturation characteristic

1. Introduction

Capacitor Voltage Transformer (CVT) is a widely used transformer in the power system. It uses a multi-level voltage reduction method to convert the input voltage into an input level signal through an electromagnetic unit. CVT mainly relies on the principle of resonance to suppress ferromagnetic resonance caused by capacitor parameters when compensating for phase difference in capacitor

voltage sharing. Its application and economy in power systems are good. The development of related electronic power rectification and inverter technologies has not only brought controllability and flexibility, but also led to the generation of variable oscillation phenomena and complex frequency characteristics of CVTs, resulting in errors and fault location problems [1, 2]. Considering the complex structure and frequency response characteristics of CVT due to changes in operating conditions and component conditions, it has multiple resonance points during high-frequency transmission. Moreover, traditional equivalent circuits of CVT often face problems such as complex data acquisition, modeling difficulties, large computational complexity, and requirements for circuit parameters when constructing broadband models, making it difficult to analyze the deviation and response of CVT models [3]. The working principle of a capacitive voltage transformer is to connect the primary winding to the voltage to be measured, and the secondary winding to the instrument or protective device, thereby reducing the measured voltage to a safe measurement range. Can convert broadband admittance models into a Π Type circuit model (Fig. 1).

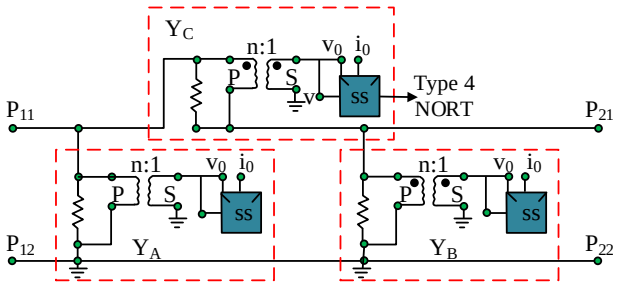

Fig. 1. CVT wideband conductor sub-model

In the figure, the Type component is grounded by default and connected to the external circuit as a transformer. In this model, the high voltage side of the transformer is connected in parallel with a resistor, and the left terminals P1 and P2 correspond to the right terminal, respectively. Therefore, the study considers constructing an electromagnetic transient model to characterize the frequency characteristics of CVT. By studying the discrete expression of parameters, frequency domain expression acquisition, model construction, and circuit construction, it aims to better simulate the response ability and characteristics of CVT under frequency excitation, in order to provide data support and reference for the operation and state detection of CVT systems. The layout structure of the research can be mainly carried out from four aspects. The first part reviews the current literature on CVT excitation deviation and power response issues. The second part starts from the frequency and saturation characteristics of transformers and reconstructs new transformers using parallel extended models. The third part is the application verification analysis of the model. The last part is a summary of the entire article.

2. Related works

Capacitive voltage transformers provide reliable voltage signals for measurement, protection, and other aspects of power systems. However, due to the complexity and nonlinearity of their internal components, they can cause error changes during transient processes after transmission.

Regarding the time step problem of power electromagnetic transients, Xu *et al*. scholars proposed a speed equivalent modeling method based on the circuit topology of dual active bridges. The results showed that this method effectively characterized details and had low accuracy loss results [4]. Mombello *et al*. scholars improved the detailed model of the voltage regulator. The results indicated that the improved model showed a good application effect in transformer case analysis [5]. Lin *et al*. scholar added a high-order nonlinear insulated gate bipolar transistor model to the electromagnetic transient device model. The results indicated that this method effectively grasped the time step characteristics between magnetic components [6]. Gao *et al*. scholars proposed a modular structure that can accelerate. The results showed that the acceleration model carried a larger order of magnitude while ensuring accuracy [7]. Ying *et al*. scholars proposed an electronic transformer based on coupling capacitors, and designed a self-maintaining duty cycle circuit to achieve load and power regulation. The circuit design had obvious anti-interference performance and high effectiveness in simulation experiments [8].

Considering the impact of stray capacitance of voltage transformers on broadband simulation performance, Shen *et al*. scholars obtained test data of transformers using non-destructive methods and established a simulation model. The experimental results indicated that the method had good consistency with the experimental data [9]. Wang *et al*. scholars quantitatively analyzed the signal interference levels of different switching devices through limited testing. The results showed that the deviation test results of the secondary voltage were less than 5% [10]. To solve the problem of conductor current attenuation in superconducting transformers affected by joint resistance, Zhang *et al*. proposed an adaptive control strategy based on learning rate radial basis functions and neural networks. The results showed that the overall system deviation under this method was less than 0.2% [11]. In response to the current difficulty of electronic transformers performing well in off calibration in power grid control systems, Hu *et al*. scholars proposed a transformer design with a passive compensation loop to reduce phase error by calculating the loop resistance and capacitance. The results indicated that the amplitude error and phase error of the transformer were less than 0.03% and 1 [12]. Chen *et al*. scholars connected an electronic load to a conventional current transformer and achieved magnetization of resistance, capacitance, and impedance based on constant magnetic flux control. The results showed that the transformer exhibited good stability in total harmonic current distortion analysis [13]. Based on the essence of magnetic field control, Cao *et al*. scholars achieved smooth motor starting by vector control and establishing a flux chain that can ensure stable amplitude and direction. The results indicated that this method effectively reduced peak current and had good application performance [14].

In summary, many scholars have used equivalent stray parameters, finite element modeling, white box models, and other methods to study the construction of CVT excitation bias and models. However, the calculation content involved in the above methods is relatively complex, and the consideration of transformer characteristics is relatively single, which cannot effectively consider parameter expression, characteristic characterization, and other aspects. Therefore, the study proposes a physical model that considers characterization characteristics to grasp the frequency and saturation characteristics of capacitive voltage transformers, in order to provide reference methods and ideas for the operation of power systems and transformer status detection, and ensure their safe operation.

3. Electromagnetic transient physical model application considering characterization characteristics to improvement of capacitive voltage transformers

Capacitive voltage transformer is an important device widely used in power systems. It mainly works through the principle of electric field coupling. However, due to the internal energy storage vision and nonlinear components of CVT, it is difficult to perform well in complex transient situations. Therefore, research is conducted to establish admittance submodels and nonlinear models based on the frequency and saturation characteristics of the transformer to characterize its performance, and to achieve coupling between these two models through two methods: admittance mutual difference and parallel expansion, thereby improving the application performance and response mechanism of capacitive voltage transformers.

3.1. Broadband admittance submodel construction based on frequency characteristics

During the operation of capacitive voltage transformers, the electric field in the primary winding is coupled to the secondary winding through insulation medium, thereby achieving voltage transmission and measurement [15]. Under common steady-state conditions, when the low-voltage side of CVT is connected to a load, in order to offset the voltage drop caused by capacitive reactance, it is necessary to ensure that the resonance relationship between the total compensation reactance and the partial voltage capacitive reactance is met. Correspondingly, it is inevitable that the transmission characteristics of CVT are more sensitive to changes in inductance and capacitive reactance [16]. Therefore, guided by the principle of two-port networks, a CVT broadband admittance submodel is constructed based on obtaining its parameter frequency response characteristics. The expression of the admittance parameter matrix is shown in Eq. (1).

$$\begin{bmatrix} Y_{11} & Y_{12} \\ Y_{12} & Y_{22} \end{bmatrix} \begin{bmatrix} I_1 \\ I_2 \end{bmatrix} = \begin{bmatrix} U_1 \\ U_2 \end{bmatrix}. \tag{1}$$

In the equation, Y represents the admittance parameters of the two ports. I_1, I_2 represent the currents of the two ports, and U_1, U_2 represent the voltages of the two ports. At the same time, the scattering parameter matrix can also better characterize the characteristics of the two ports, which can be defined as Eq. (2).

$$\begin{bmatrix} b_1 \\ b_2 \end{bmatrix} = \begin{bmatrix} S_{11} & S_{12} \\ S_{21} & S_{22} \end{bmatrix} \begin{bmatrix} a_1 \\ a_2 \end{bmatrix}. \tag{2}$$

In Eq. (2), S is the scattering parameter. a_1, a_2 represent the normalized incident scattering variables of the port, and b_1, b_2 are the reflection scattering variables of port 2. The original black box model ignored the internal current information of the CVT when constructing a broadband model. Therefore, the study used port voltage and current as excitation responses and utilized admittance parameters to construct the CVT model. At the same time, considering the short existence time of the high-voltage side current of the CVT and the high instantaneous power, the frequency sweep method was used to measure the port parameters [17]. Equation (3) is the admittance parameter matrix calculated based on scattering parameters.

$$Y(\omega) = \begin{bmatrix} Y_{11}(\omega) & Y_{12}(\omega) \\ Y_{12}(\omega) & Y_{22}(\omega) \end{bmatrix}. \tag{3}$$

In Eq. (3), 1, 2 represent the ports. As the admittance parameters under scattering parameter calculation are discrete data points, it is difficult to conduct simulation analysis. Therefore, the study uses vector matching method to achieve parameter fitting, transforming it into the form of a rational functional sum, as shown in Eq. (4).

$$f(s) \approx \sum_{n=1}^{N} \frac{c_n}{s - a_n} + d + es. \tag{4}$$

In Eq. (4), c_n, a_n represent the residue and poles of the function. d, e are the real constant parameters, s indicates the S parameter and N is the fitting order. The vector matching method utilizes the least squares method to optimize two linear equations within the specified frequency range. Due to the existence of multiple resonant frequency points in the broadband response characteristics of CVT, complex poles should be taken into account when selecting initial poles, and their values can be determined by constructing discrete data into linear functions or linear equations [18]. By performing a reverse pull transformation on the fitted admittance parameter equation and designing the circuit with discrete data points at fixed time steps, the discrete state space equation in the time domain can be obtained, as shown in Eq. (5).

$$\begin{cases} \dfrac{x_{k+1} - x_k}{h} = A\dfrac{x_{k+1} + x_k}{2} + B\dfrac{u_{k+1} + u_k}{2} \\ i_{k+1} = Cx_{k+1} + I_{k+1} \end{cases} . \tag{5}$$

In Eq. (5), A represents the $N \times N$ diagonal matrix. B represents the $N \times 1$ column vector. C represents the $1 \times N$ row vector. k represents the time. h represents a fixed time step, represents the unit matrix. x_k represents the state variable at time k. u_k is the voltage at time k, and i_k is the relay current at time k. The equation can be rearranged and simplified using the central differential method, and then the parameter results can be obtained by substitution and organization.

3.2. Nonlinear models' construction based on saturation characteristics

The broadband admittance model can effectively obtain small signal excitation of equipment, but it does not pay attention to the complex nonlinearity of the internal iron core of CVT based on characterizing the frequency characteristics of CVT, and there is no corresponding relationship between the intermediate transformer model and the physical structure of the transformer [19]. Therefore, based on the dual transformation relationship of the electromagnetic circuit, a dual model of the transformer under the excitation branch is proposed, and its parameters are identified and allocated. The electromagnetic duality relationship can be represented as Fig. 2.

From the perspective of component relationships, the magnetic electromotive force and magnetic resistance in the magnetic circuit can be converted into the current source and inductance in the circuit. From the perspective of topological correspondence, the mesh and nodes in the magnetic circuit are in opposition to the circuit, and the series parallel connection of the magnetic resistance can be equivalent to the parallel series connection of the inductance. Randomly, a dual model can be constructed based on the above correspondence, resulting in Fig. 3.

During the design process, each magnetic circuit component passes through the connection line and the number of connections at the node is at least twice. Based on the physical structure of CVT, a low-frequency nonlinear sub model of CVT under the electromagnetic dual model can be constructed, as shown in Fig. 4.

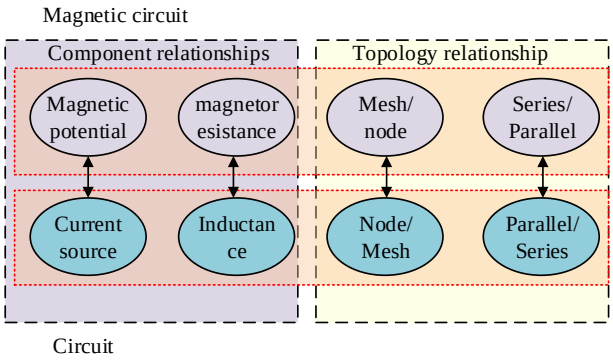

Fig. 2. Schematic diagram of electromagnetic dyadic relationship conversion

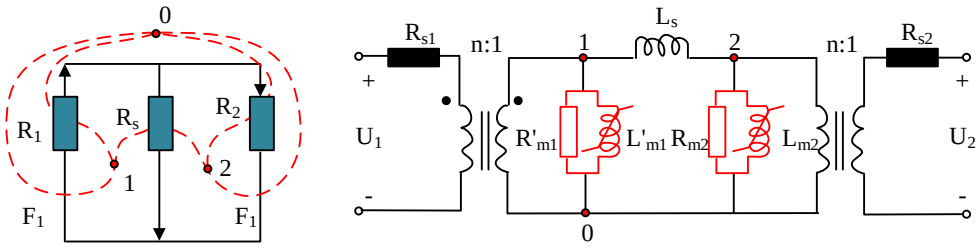

(a) Equivalent magnetic circuit (b) Equivalent dyadic circuit

Fig. 3. Equivalent magnetic circuit and dyadic circuit structure of an intermediate transformer

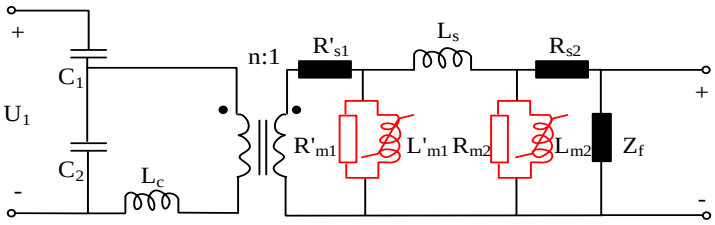

Fig. 4. Low-frequency nonlinear sub-model of CVT under the battery dyadic principle

There are differences in the excitation characteristics of intermediate transformers at different iron cores and positions, therefore, research is conducted on the electromagnetic dual model of CVT intermediate transformers for deep saturation parameter testing. Firstly, the concept of inductance is introduced for the saturation characteristics of transformers, and its mathematical expression is shown in Eq. (6).

$$\begin{cases} L = \dfrac{\psi}{I} \\ L' = \dfrac{\mathrm{d}\psi}{\mathrm{d}I} \end{cases} . \tag{6}$$

In Eq. (6), L represents the static inductance. ψ represents the flux linkage, and L' represents the incremental inductance. When the saturation degree of the intermediate transformer core deepens, both types of inductors will show a decreasing trend and the incremental inductance will be more obvious. The increase in DC voltage output value will excite the transformer core to exhibit different saturation depths, so the characterization information extraction of its process can be achieved by recording data at different saturation points [20]. The current distribution of the excitation branch can be expressed as Eq. (7).

$$\begin{cases} I'_{m1}(q) + I_{m2}(q) = I_{dc}(q) \\ I'_{m1}(q) \cdot L_{m1}(q) = I_{m2}(q) \cdot [L_s + L_{m2}(q)] \end{cases} . \tag{7}$$

In Eq. (7), q represents the number of saturation test points. I'_{m1}, I_{m2}, represent the excitation currents on the high-voltage and low-voltage sides of the intermediate transformer, and L_{m1}, L_{m2} represent the deep saturation inductances on both sides of the transformer. The operating conditions of capacitive voltage transformers are relatively complex, and their electromagnetic transient involves a lot of content. Therefore, based on the model in the first section, a broadband nonlinear model of CVT in a combined form is constructed. By utilizing the extended form of parallel circuits, the model combination is achieved, as shown in Fig. 5.

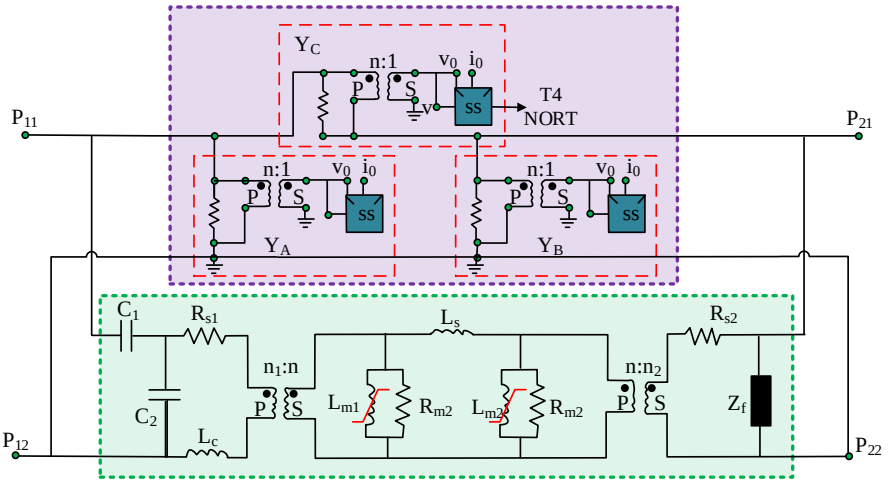

Fig. 5. CVT wideband nonlinear model

At the same time, in order to reduce the coupling error of the model during the expansion process, linear processing of the components of the nonlinear submodel is studied using the rated operating conditions parameters, and the admittance parameters of the linear model are calculated to obtain Eq. (8).

$$Y_{50}(\omega) = \begin{bmatrix} \dfrac{I'_1}{l^2 U'_1} \Big| U_2 = 0 & \dfrac{I'_1}{l U_2} \Big| U'_1 = 0 \\ \dfrac{I_2}{l U'_1} \Big| U_2 = 0 & \dfrac{I_2}{U_2} \Big| U'_1 = 0 \end{bmatrix} . \tag{8}$$

In Eq. (8), l is the transformer ratio. U_1', I_1' are the voltage and current on the high-voltage side of the CVT on the low-voltage side, and U_2, I_2 are the voltage and current on the low-voltage side of the CVT. Obtain the broadband admittance parameters through mutual difference in admittance, as shown in Eq. (9).

$$Y(\omega) = Y_w(\omega) - Y_{50}(\omega). \tag{9}$$

In Eq. (9), $Y_w(\omega)$ represents the admittance matrix of the originally determined four ports under the calculation of scattering parameters.

4. Deviation response application results analysis of capacitive voltage transformer under the physical model of electromagnetic transient

The response speed and accuracy of capacitive voltage transformers in power systems directly affected the operation and protection of the system, and the excitation process in the power system was affected by factors such as load changes and rapid changes in line current. The study utilized electromagnetic transient physical models to simulate operating conditions error and analyze power response of capacitive voltage transformers. To better validate the effectiveness of the proposed parallel transformer model, the TYD35/3-0.01HF model CVT was used as the experimental object for application analysis. The rated voltage of this CVT model was $35/\sqrt{3}$ with a rated change of 350, and the transformation ratio of the intermediate transformer was $100/\sqrt{3}$. Some parameters of the CVT nonlinear submodel were tested through open circuit and short circuit tests, where the submodel and equivalent parameters of circuit components are shown in Table 1.

Table 1. Nonlinear model parameters and component equivalent parameters

Parametric	**Note**	
C_1	19 930 pF	
C_2	19 940 pF	
L_c	243 H	
L'_s	1.17 mH	
R'_{s1}	0.038 Ω	
R_{s2}	0.035 Ω	
Equivalent components	Note	
Power side resistor	Series resistors	60 Ω
Transformer	Inductors and inlets	20 mH
	Capacitance	2 000 pF
Bushing	Ground capacitance	300 pH
Capacitive load	Concentration capacitance	5 000 pF
Grounding at load	Resistance to ground	3 Ω

Parameter identification had a significant impact on the performance of capacitive voltage transformers, where admittance parameters described the degree of response of circuit components to voltage and current changes. The study utilized the calibrated network analyzer E5061B for CVT high and low voltage side analysis, and obtained the scattering parameters of the 6 500 frequency points and their corresponding logarithmic distribution within the range of 5 Hz-1 MHz. The scattering parameter matrix and admittance were obtained, as shown in Fig. 6.

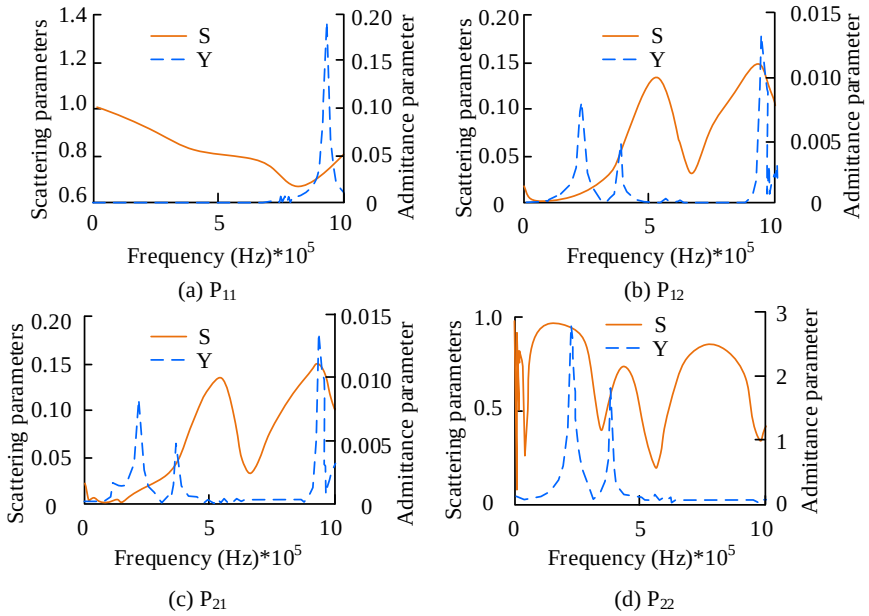

Fig. 6. Amplitude characteristics of circuit scattering parameters and conductance parameters

In Fig. 6, the scattering parameters indicated that the reflection loss S11 value of the input and output ports was basically less than 1.0, and its overall variation value was small. However, the coefficient curve of S21 showed multiple peaks. At the same time, there was at least one peak in the amplitude of the admittance parameter, and the maximum values of the four ports reached 1.32, 0.17, 0.17, and 0.93 respectively, all of which exhibited strong current responsiveness. Subsequently, low-frequency inrush current experiments and impulse voltage experiments were designed to validate the simulation model. The signal sources selected by the research institute were a Tektronix AFG3011 generator and AE TECHRON 7548 power amplifier. The inrush current experiment applied a sine wave on the low-voltage side of the CVT, and recorded the low-voltage side current and voltage during the high-voltage side open circuit process. The voltage closing phase was 0, and demagnetization treatment was performed during each experiment process. The results are shown in Fig. 7.

In Fig. 7, the current simulation error between the first peak amplitude (52.42 A) displayed by the measured current curve of CVT and the simulation result (51.37 A) is less than 2%, while the error between the simulation result and the measured value under traditional transformers is much greater than 50%. The voltage results show that the curve direction between the simulated value

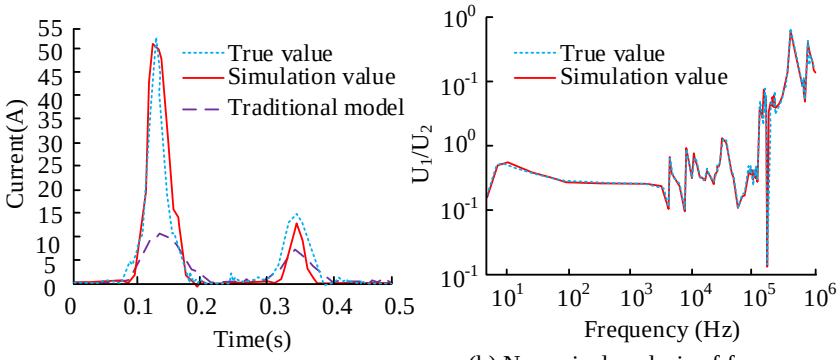

(a) CVT current simulation results

(b) Numerical analysis of frequency response of CVT voltage transfer function

Fig. 7. Comparison of results of current waveform and voltage transfer frequency response

and the actual value is basically consistent, with a deviation value of less than 1%. The setup of the impulse voltage signal source was similar to the surge current experiment. The current and response characterization results of the parallel circuit coupling model under voltage transmission frequency are shown in Fig. 8.

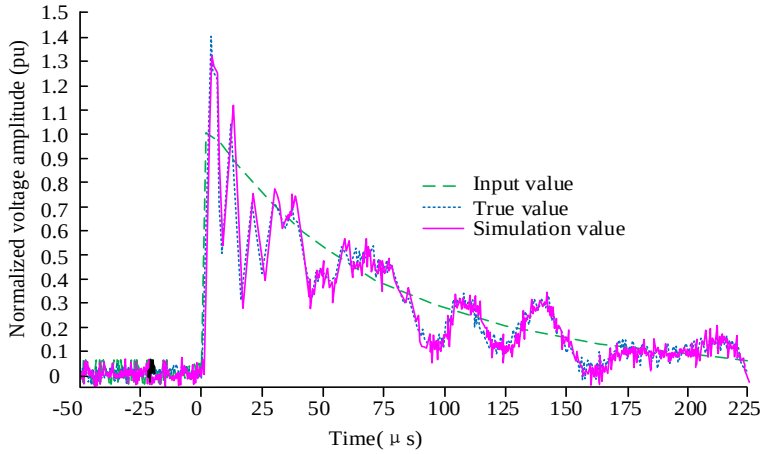

Fig. 8. Variation of CVT voltage waveform under lightning experiment

In Fig. 8, the input voltage value showed a downward trend when the time was greater than 0 μs. The simulated response curve in the figure exhibited several peaks, and the difference between the first peak value and the actual test result was 0.043 pu, with an overall error result of 3.12%. This indicated that the proposed model effectively normalized the input voltage and exhibited its electromagnetic transient characteristics under wideband conditions. When the CVT system failed, the primary and secondary voltages experienced transient response. Therefore, the transient errors during this process were analyzed, and the results are shown in Fig. 9.

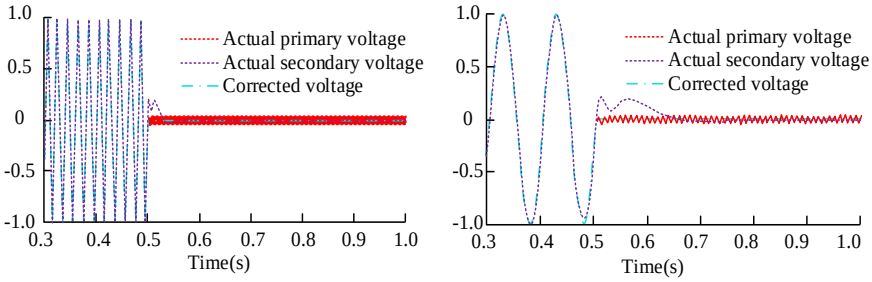

Fig. 9. Comparison graph before and after voltage correction

When a transient response occurs, the primary voltage will immediately become 0, while the secondary voltage needs to undergo a decay process to reach 0. In Fig. 9, Fig. 9(a) represents the comparison between the actual primary and secondary voltages of the CVTC and the corrected primary voltage, and Fig. 9(b) represents the local amplification result of the voltage in Fig. 9(a). When a short-circuit fault occurs in the primary side of the CVTC, the curve of the corrected voltage results changes smoothly at different times, and the agreement between its voltage variation and the actual results is greater than 98%. When a transient response occurs, the primary voltage will immediately become 0, while the secondary voltage needs to undergo a decay process to reach 0. The secondary voltage of the results in Fig. 9(b) has a good tracking relationship with the actual primary voltage after the time is greater than 0.53 s. The primary voltage of the results in Fig. 9(c) has a good tracking relationship with the actual primary voltage. The reason that the calibrated primary voltage does not become zero immediately may be due to the iterative solution error in the CVT rated parameters when the simulation is performed. Considering the differences in signal data displayed by electronic current transformers in different electromagnetic environments, strong electromagnetic interference caused errors in the output signal. Therefore, the study aimed to investigate the power output characteristics of the proposed electronic transformer under complex electromagnetic environment conditions. The output voltage was analyzed by setting two conditions: circuit breaker disconnection and arc reignition, and the results are shown in Fig. 10.

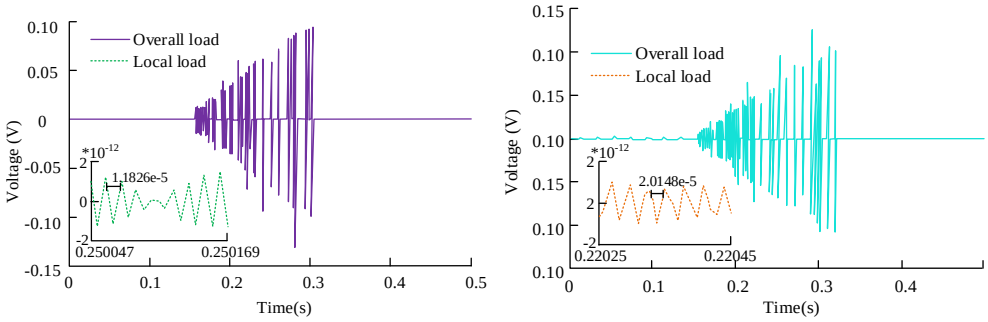

(a) Voltage load condition of CVT output terminal before application

(b) Voltage load situation of CVT output terminal after application

Fig. 10. Equivalent magnetic circuit and dyadic circuit structure of an intermediate transformer

In Fig. 10, the cycle of the proposed transformer in the output voltage load was mainly concentrated in the range of 0.15 s to 0.33 s, and its maximum harmonic frequency was 2.0148e-5, which was much higher than the 0.15 s to 0.30 s and 1.1826e-5 of traditional CVT, indicating that it had better high-frequency response ability and effectively determined signal components. The harmonic situation of the voltage supply terminal and load terminal under the arc reignition condition was analyzed, and the results are shown in Fig. 11.

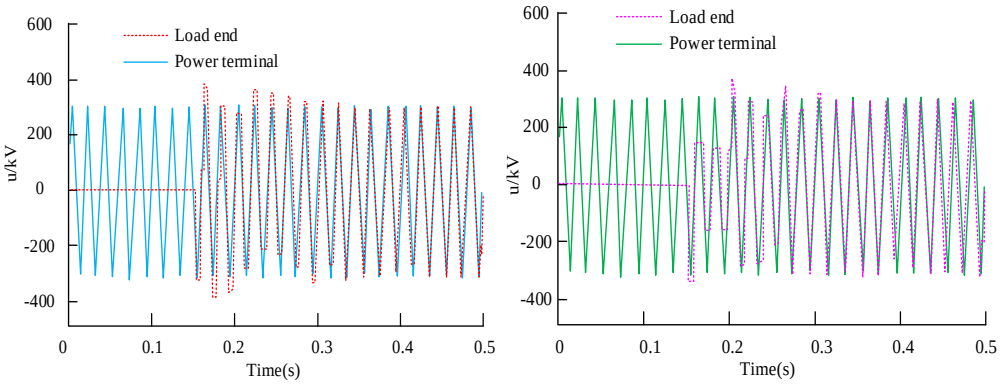

(a) Traditional capacitive voltage transformer (b) Improving capacitive voltage transformers

Fig. 11. Supply-side and load cases of CVT output voltage under arc re-ignition conditions

In Fig. 11, under the condition of arc reignition, the load terminal waveform of the transformer almost coincided with the power terminal waveform, and the overall change was relatively stable. However, the load voltage shown by traditional CVT fluctuated, accompanied by significant harmonics. The harmonic error reached 1.73% between 0.15s and 0.31s, and the voltage curve gradually stabilized later.

5. Conclusion

Studying the excitation deviation and power response performance of CVT is important for maintaining the stability and reliability of power systems. Therefore, characterizing the properties of CVT and analyzing their electromagnetic transient characteristics are crucial for improving their performance. The results showed that the improved CVT had lower transmission losses and stronger power response with its scattering parameters and admittance values being 1.32, 0.17, 0.17, and 0.93 for each port. During the experiment, the error between the measured first peak amplitude (52.42 A) of the CVT surge current curve and the simulated result (51.37 A) was less than 2%, and its voltage curve was consistent with the actual value. In contrast, the error between the traditional CVT simulation result and the actual measurement was greater than 50%. The difference between the simulated response result and the actual result's first peak value was 0.043 pu, with an overall error of 3.12% and multiple peaks. When a short-circuit fault occurred in the CVT, the improved CVT had smaller transient errors, and the consistency between the corrected primary voltage result and the actual primary voltage result was greater than 98%,

with no significant load-side fluctuations. This was different from the 1.73% harmonic error of traditional CVT from 0.15 s to 0.31 s. The proposed improved CVT can explain its characterization properties well, effectively reduce excitation deviation, and improve the accuracy and sensitivity of power response. Future research should focus on studying the wideband nonlinear model under multiple factors such as frequency and environment.

References

[1] Frigo G., Agustoni M., *Calibration of a digital current transformer measuring bridge: Metrological challenges and uncertainty contributions*, Metrology, vol. 1, no. 2, pp. 93–106 (2021), DOI: 10.3390/metrology1020007.

[2] Sun K., Qiu W., Yao W., You S., Yin H., Liu Y., *Frequency injection based HVDC attack-defense control via squeeze-excitation double CNN*, IEEE Transactions on Power Systems, vol. 36, no. 6, pp. 5305–5316 (2021), DOI: 10.1109/TPWRS.2021.3078770.

[3] Wang J., Chen W., *Output characteristics analysis of energy harvesting current transformer*, IEEE Sensors Journal, vol. 21, no. 20, pp. 22595–22602 (2021), DOI: 10.1109/JSEN.2021.3107864.

[4] Xu J., Gao C., Ding J., Shi X., Feng M., Zhao C., Ding H., *High-speed electromagnetic transient (EMT) equivalent modelling of power electronic transformers*, IEEE Transactions on Power Delivery, vol. 36, no. 2, pp. 975–986 (2020), DOI: 10.1109/TPWRD.2020.2998498.

[5] Mombello E.E., Portillo Á., Flórez G.A.D., *New state-space white-box transformer model for the calculation of electromagnetic transients*, IEEE Transactions on Power Delivery, vol. 36, no. 5, pp. 2615–2624 (2020), DOI: 10.1109/TPWRD.2020.3023824.

[6] Lin N., Liu P., Dinavahi V., *Component-level thermo-electromagnetic nonlinear transient finite element modeling of solid-state transformer for DC grid studies*, IEEE Transactions on Industrial Electronics, vol. 68, no. 2, pp. 938–948 (2020), DOI: 10.1109/TIE.2020.2967687.

[7] Gao C., Feng M., Ding J., Zhang H., Xu J.Z., Zhao C.Y., *Accelerated electromagnetic transient (EMT) equivalent model of solid-state transformer*, IEEE Journal of Emerging and Selected Topics in Power Electronics, vol. 10, no. 4, pp. 3721−3732 (2021), DOI: 10.1109/jestpe.2021.3094278.

[8] Ying L., Bing L., FangFang S., Gao H., Huang L., Chen X., *Energy harvest system research for high precision electronic voltage transformer based on coupling capacitance*, Transactions on Electrical and Electronic Materials, vol. 23, no. 6, pp. 624–631 (2022), DOI: 10.1007/s42341-022-00395-8.

[9] Shen Z., Wang J., Yan X., Zhao P.C., Cui M., Xu C.J., Cao X., *A method for extracting stray capacitance and hysteresis curves of potential transformers based on frequency referring*, IEEE Transactions on Power Delivery, vol. 37, no. 3, pp. 1897–1905 (2021), DOI: 10.1109/TPWRD.2021.3100602.

[10] Wang Q., Fu C., Chu F., Tong Y., Wang X.Z., Ye G.X., Wu X., *A quantitative research on the level of disturbance to secondary signal ports of electronic voltage transformers under the operation of gas-insulated switchgear*, High Voltage, vol. 7, no. 1, pp. 165–175 (2022), DOI: 10.1049/hve2.12121.

[11] Zhang S., Liu H., Liu F., Ma H.J., Shi Y, Gao P., Zhou C., Qin J.G., *Research on excitation current control system of the 50 kA superconducting transformer*, IEEE Transactions on Applied Superconductivity, vol. 31, no. 8, pp. 1–4 (2021), DOI: 10.1109/TASC.2021.3108756.

[12] Hu H., Xu Y., Wu X., Lin F.C., Xiao X., Lei M., *Passive-compensation clamp-on two-stage current transformer for online calibration*, IET Science, Measurement and Technology, vol. 15, no. 9, pp. 730–737 (2021), DOI: 10.1049/smt2.12073.

[13] Chen F., Yang C., Guo Z., Wang Y., Ma X., *A magnetically controlled current transformer for stable energy harvesting*, IEEE Transactions on Power Delivery, vol. 38, no. 1, pp. 212–221 (2022), DOI: 10.1109/TPWRD.2022.3184327.

[14] Cao Z., Shi J., Fan B., *Induction motor pre-excitation starting based on vector control with flux linkage deviation decoupling*, Journal of Vibroengineering, vol. 23, no. 3, pp. 728–743 (2021), DOI: 10.21595/jve.2020.21635.

[15] Zhu T., Shao Z., Nie Y., *Stray capacitances calculation and harmonic measurement of capacitor voltage transformer*, International Journal of Numerical Modelling: Electronic Networks, Devices and Fields, vol. 35, no. 6, e3024 (2022), DOI: 10.1002/jnm.3024.

[16] Sima W., Peng D., Yang M., Sun P., Zhou B., Xiong Z., *Reversible wideband hybrid model of two-winding transformer including the core nonlinearity and EMTP implementation*, IEEE Transactions on Industrial Electronics, vol. 68, no. 4, pp. 3159–3169 (2020), DOI: 10.1109/TIE.2020.2977544.

[17] Lesniewska E., Olak J., *Analysis of the operation of cascade current transformers for measurements of short-circuit currents with a non-periodic component with a large time constant of its decay*, Energies, vol. 15, no. 8, pp. 2924–2925 (2022), DOI: 10.3390/en15082925.

[18] Kraszewski W., Syrek P., Mitoraj M., *Methods of ferroresonance mitigation in voltage transformers in a 30 kV power supply network*, Energies, vol. 15, no. 24, 9516 (2022), DOI: 10.3390/en15249516.

[19] John Y.M., Sanusi A., Yusuf I., Modibbo U.M., *Reliability analysis of multi-hardware–software system with failure interaction*, Journal of Computational and Cognitive Engineering, vol. 2, no. 1, pp. 38–46 (2023), DOI: 10.47852/bonviewJCCE2202216.

[20] Waziri T.A., Yakasai B.M., *Assessment of some proposed replacement models involving moderate fix-up*, Journal of Computational and Cognitive Engineering, vol. 2, no. 1, pp. 28–37 (2023), DOI: 10.47852/bonviewJCCE2202150.